

# Meson spectroscopy, resonances and scattering on the lattice

Christopher E. Thomas<sup>1,a</sup>

(on behalf of the Hadron Spectrum Collaboration)

<sup>1</sup>DAMTP, University of Cambridge, Centre for Mathematical Sciences, Wilberforce Road, Cambridge, CB3 0WA, UK

**Abstract.** I discuss some recent progress in studying the spectra of mesons using first-principles lattice QCD calculations. In particular, I highlight some new results on resonances, near-threshold states and related scattering phenomena – this is an area which is very interesting experimentally and theoretically and where we have made significant advances in the last few years. I conclude with an outlook on future prospects.

## 1 Introduction

Over the last decade or so there has been renewed interest in hadron spectroscopy driven by a wealth of experimental data. Amongst other things, a number of ‘puzzling’ states have been observed and, as has been reviewed elsewhere at this conference [1, 2], these are the subject of theoretical work and ongoing experimental investigations. Examples include various charmonium and bottomonium-like structures (“X, Y, Z’s”) and the charm-strange  $D_{s0}(2317)$ . There has been a lot of speculation as to their nature and possibilities put forward include tetraquarks (containing two quarks and two antiquarks), molecular states of hadrons, hadro-quarkonia and hybrid mesons (where the gluonic field is excited). States with exotic quantum numbers, i.e. those which cannot arise from solely a quark-antiquark pair, are particularly interesting because they are a smoking gun for physics beyond a model of a quark and an antiquark moving in a potential. For example, exotic flavour states (such as charged charmonium and bottomonium-like states) or exotic spin ( $J$ ), parity ( $P$ ), charge-conjugation ( $C$ ) combinations (e.g.  $J^{PC} = 0^{--}, 0^{+-}, 1^{-+}, 2^{+-}$ ).

A method to perform first-principles calculations of the spectra and properties of hadrons is provided by lattice QCD: four-dimensional space-time is discretised on a finite four-dimensional hypercubic lattice and the calculation of quantities in the path integral formulation then becomes an ordinary (but very large) integration problem. If a Euclidean (imaginary-time) space-time metric is used, the integrals can be evaluated effectively using importance-sampling Monte Carlo methods. The masses and other properties of hadrons are then extracted from correlation functions involving interpolating operators constructed from quark and gluon fields. Calculations of the low-lying spectrum of hadrons have long been benchmarks of lattice methods and there are very accurate results which include detailed considerations of the various systematic uncertainties such as those arising from working at a finite lattice spacing and in a finite volume – see for example Refs. [3, 4]. On the other hand, in the last few years there has been significant progress in using lattice QCD to study excited hadrons. These

<sup>a</sup>e-mail: c.e.thomas@damtp.cam.ac.uk

calculations do not usually have precise control over all the systematic uncertainties and often have unphysically-heavy light quarks. Although I will note the corresponding pion masses,  $m_\pi$ , details of the calculations will not be given here and I refer to the references for further information.

Most hadrons are unstable with respect to the strong interaction and appear as resonances in the scattering of two or more lighter hadrons. In particular, many of the puzzling states appear close to or above the threshold for strong decay – this must be taken into account in theoretical approaches and experimentally the effects of many coupled-channels (including many-hadron final states) often need to be disentangled. In recent years there has been significant progress in using lattice QCD to study resonances, near-threshold states and related scattering phenomena and, concentrating on results that have appeared in the last two years or so, I will review some of this work in these proceedings.

After a brief description of some of the lattice QCD methodology in Section 2, in Section 3 I discuss calculations of the  $\rho$  resonance in  $\pi\pi$  scattering. Some other channels relevant for light and strange mesons are discussed in Section 4 followed by heavy-light and charmonium-like resonances in Section 5. I conclude in Section 6 with an outlook.

## 2 Excited spectroscopy and scattering in lattice QCD

In lattice QCD the discrete spectrum of states in a finite volume follows from analysing the dependence of two-point correlation functions,

$$C_{ij}(t) = \langle 0 | O_i(t) O_j^\dagger(0) | 0 \rangle,$$

on the time separation  $t$ . Here the interpolating operator  $O_j^\dagger(0)$  creates the states of interest at time 0 and  $O_i(t)$  annihilates them at time  $t$  – all states with the quantum numbers of the operators contribute to the correlation function. The variational method [5–7] enables excited states to be extracted reliably: a matrix of correlation functions involving a basis of  $N$  operators with the required quantum numbers is computed,  $C_{ij}(t)$ , where  $i, j = 1, 2, \dots, N$ . A generalised eigenvalue problem,

$$C_{ij}(t) v_j^{(n)} = \lambda^{(n)}(t) C_{ij}(t_0) v_j^{(n)},$$

is then solved for an appropriate reference time  $t_0$ . The time dependence of an eigenvalue  $\lambda^{(n)}(t)$  is related to the energy of the  $n$ 'th state and the eigenvector,  $v_i^{(n)}$ , is related to the operator-state overlap,  $Z_i^{(n)} \equiv \langle 0 | O_i | n \rangle$ ; these overlaps can be used to probe the structure of states. The eigenvectors also give the optimal (in a variational sense) linear combination of operators to create the  $n$ 'th state. To accurately determine the spectrum, the basis of operators must have a sufficiently wide range of structures to disentangle the various states that appear.

Although it is not possible to compute scattering properties directly in the Euclidean formulation of lattice QCD, the Lüscher method [8–10] and its extensions [11–19] allow indirect access to *infinite-volume* scattering amplitudes from *finite-volume* spectra, at least in the case of any number of two-hadron coupled channels. For elastic scattering, there is a one-to-one correspondence<sup>1</sup> between an energy level with centre-of-mass energy  $E_{\text{cm}}$  and the scattering phase shift  $\delta$  at  $E_{\text{cm}}$  or equivalently the scattering  $t$ -matrix,  $t(E_{\text{cm}})$ . For coupled-channel two-hadron scattering, extracting an energy level  $E_{\text{cm}}$  constrains the scattering  $t$ -matrix at  $E_{\text{cm}}$  but this is in general an under-constrained problem. For example, with two coupled channels there are three energy-dependent parameters but only one constraint at each  $E_{\text{cm}}$ . One solution is to parameterize the  $E_{\text{cm}}$ -dependence of the  $t$ -matrix with a

<sup>1</sup>ignoring complications arising from the mixing of partial waves due to the reduced symmetry of a finite box which we will not discuss here

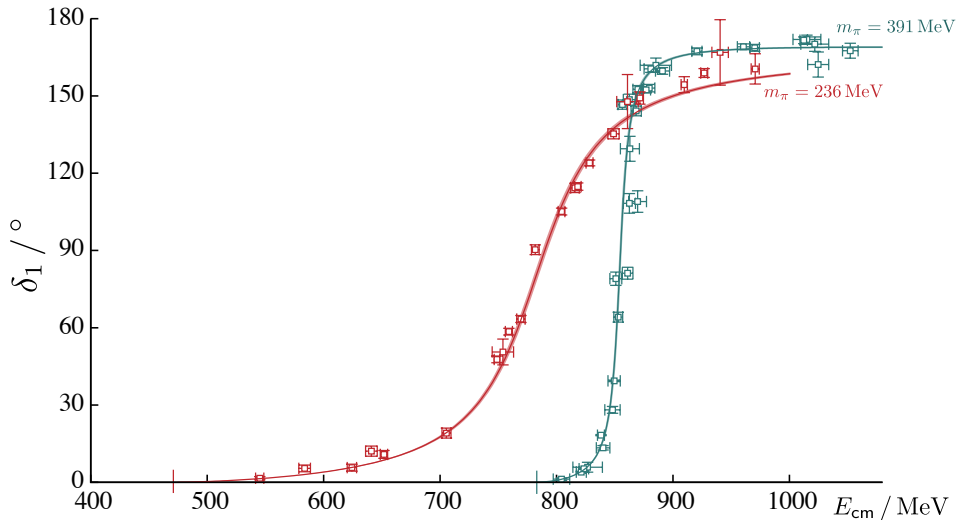


**Figure 1.** From Ref. [27]. The  $P$ -wave  $I = 1$   $\pi\pi$  elastic scattering phase shift as a function of cm-frame energy ( $E_{\text{cm}}$ ) plotted from  $\pi\pi$  threshold to the inelastic  $K\bar{K}$  threshold, from dynamical lattice QCD calculations with  $m_\pi \approx 240$  MeV [27] and  $m_\pi \approx 390$  MeV [31]. Points are from an energy-level by energy-level analysis and the curves are from a relativistic Breit Wigner parameterization as described in [27].

relatively small number of parameters – the spectrum resulting from this  $t$ -matrix is fit to the computed spectrum by varying these parameters. With the  $t$ -matrix in hand, its singularity structure can be investigated to determine the bound state and resonant content. The former corresponds to a pole below threshold on the real axis of the physical Riemann sheet, whereas the latter corresponds to poles away from the real axis on unphysical sheets. The scattering formalism was discussed in more detail elsewhere at this conference [20].

### 3 The $\rho$ resonance in $\pi\pi$ scattering

One of the simplest resonances, and the one that has attracted the most initial attention from lattice QCD [21–25], is the  $\rho(770)$  which appears in  $\pi\pi$  scattering in  $L = 1$  ( $P$ -wave) with  $J^{PC} = 1^{--}$  and isospin  $I = 1$ ; empirically the  $\rho$  decays almost entirely to  $\pi\pi$  [26]. The results of a recent lattice QCD calculation [27] of the elastic  $I = 1$   $\pi\pi$  scattering phase shift by the Hadron Spectrum Collaboration (HSC) are shown in Fig. 1. The lattices are anisotropic with a temporal lattice spacing,  $a_t$ , finer than the spatial lattice spacing,  $a_s \approx 0.12$  fm, and  $\xi \equiv a_s/a_t \approx 3.5$ . The computations have dynamical strange and degenerate up and down quarks, “ $N_f = 2 + 1$ ”, corresponding to  $m_\pi \approx 240$  MeV, and the plot also shows results from an earlier calculation with  $m_\pi \approx 390$  MeV. A range of techniques were used to compute extensive excited finite-volume spectra with a high statistical precision. Correlation matrices were calculated with large bases of carefully-constructed fermion-bilinear [28, 29] and multi-hadron interpolating operators [30] and then analysed using the variational method. The resulting spectra enabled the energy dependence of the scattering phase shift to be mapped out in detail via the Lüscher method.

The figure shows convincingly the rapid rise in the phase shift from 0 through 90 to 180 that is expected in the presence of a single isolated resonance. The resonance mass ( $M_R = 790 \pm 2$  MeV) is not too different from experiment ( $775.49 \pm 0.3$  MeV) but the width is significantly smaller ( $\Gamma = 87 \pm 2$  MeV compared to  $149.1 \pm 0.8$  MeV experimentally). This is simply because the pion mass in this study is larger than the physical value and so the phase space for decay is reduced. The coupling,  $g$ , with the phase space factor divided out, defined by  $\Gamma = \frac{g^2}{6\pi} \frac{p_{\text{cm}}^3}{M_R}$ , where  $p_{\text{cm}}$  is the cm-frame scattering momentum, shows little dependence on  $m_\pi$  and is in reasonable agreement with the experimental value. Calculations by another group on the same lattices using slightly different techniques are presented in Ref. [32].

Ref. [27] also extends the analysis to the energy region above  $K\bar{K}$  threshold and considers coupled  $\pi\pi$ ,  $K\bar{K}$  scattering. It is found that there is negligible coupling between the channels in the energy range explored.

The RQCD Collaboration have recently studied the  $\rho$  resonance with  $m_\pi \approx 150$  MeV, close to the physical value [33]. However, in these “ $N_f = 2$ ” computations only the light up and down quarks were dynamical whereas the strange quarks were quenched (not present in the sea). As can be seen from the comparison of different lattice QCD results in Ref. [33], the resonance mass is sensitive to whether or not the strange quarks are quenched (unlike  $g$  which is insensitive to this and to  $m_\pi$ ). The same effect was observed in recent  $N_f = 2$  computations by Guo et. al. [34] with  $m_\pi = 226$  and 315 MeV, and was discussed in Ref. [35] and at this conference [36].

Going beyond the resonance mass and width, recently the form factor of an unstable hadron has been calculated for the first time in lattice QCD using generalizations [37–39] of the formalism developed by Lellouch and Lüscher [40]. From computations of the  $\pi\pi \rightarrow \pi\gamma^*$  transition amplitude, the resonant  $\rho \rightarrow \pi\gamma^*$  transition form factor and the radiative decay width were extracted as discussed in Refs. [41, 42] and presented at this conference [20].

## 4 Other scattering channels relevant for light and strange mesons

Moving to other scattering channels relevant for light and strange mesons, using a similar setup to that described above with  $m_\pi \approx 390$  MeV and three lattice volumes, the HSC investigated coupled-channel  $K\pi$ ,  $K\eta$  scattering with  $I = 1/2$  [43, 44], the first study of coupled-channel scattering on the lattice. In total 73 energy levels were extracted and these enabled the energy dependence of the scattering matrix to be mapped out. A number of interesting features emerged including a broad  $J^P = 0^+$  scalar resonance in  $S$ -wave [c.f. the  $K_0^*(1430)$ ], a  $P$ -wave  $1^-$  vector bound state [c.f. the  $K^*(892)$ ], a narrow  $2^+$  tensor resonance in  $D$ -wave [c.f. the  $K_2^*(1430)$ ] and a suggestion that the  $\kappa$ , a scalar resonance with physical-mass light quarks, corresponds to a virtual bound state<sup>2</sup> when  $m_\pi \approx 390$  MeV. The latter observation is consistent with how the  $\kappa$  behaves in unitarised chiral perturbation theory as the  $\pi$  mass is varied [45]. The exotic-flavour  $I = 3/2$   $K\pi$  channel was also studied.

The RQCD Collaboration have studied  $P$ -wave elastic  $K\pi$  scattering in a  $N_f = 2$  calculation with light quarks corresponding to  $m_\pi \approx 150$  MeV [33]. They find a vector resonance, consistent with the expectation that the bound state found by the HSC with  $m_\pi \approx 390$  MeV becomes a resonance as the light-quark masses are reduced.

The HSC have also studied coupled  $\pi\eta$ ,  $K\bar{K}$ ,  $\pi\eta'$  scattering in  $I = 1$  with  $m_\pi \approx 390$  MeV on three lattice volumes [46]. The  $S$ -wave coupled-channel  $\pi\eta$ ,  $K\bar{K}$  scattering amplitudes constrained by 47 energy levels are shown in Fig. 2. Here the phase shifts,  $\delta_i$ , and inelasticity,  $\eta$ , are defined in terms of

<sup>2</sup>a pole below threshold on the real axis of an unphysical Riemann sheet

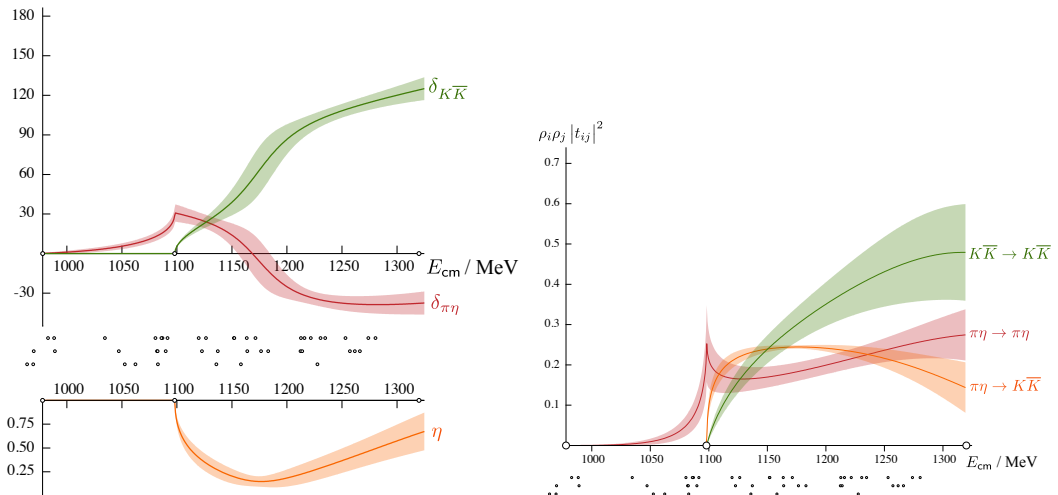


**Figure 2.** From Ref. [46]. The S-wave  $I = 1$   $\pi\eta$ ,  $K\bar{K}$  coupled-channel scattering amplitudes ( $J^{PC} = 0^{++}$ ) from a lattice calculation with  $m_\pi \approx 390$  MeV. Left panel shows phase shifts,  $\delta_i$ , and inelasticity,  $\eta$ , and the right panel shows quantities proportional to cross sections. Open circles on the horizontal axis indicate  $\pi\eta$ ,  $K\bar{K}$  and  $\pi\eta'$  thresholds. The dots below the figures show energy levels used to constrain the amplitudes.

elements of the  $t$ -matrix,<sup>3</sup>

$$t_{ij} = \begin{cases} \frac{\eta e^{2i\delta_i} - 1}{2i\rho_i} & (i = j) \\ \frac{\sqrt{1-\eta^2} e^{i(\delta_i + \delta_j)}}{2\sqrt{\rho_i \rho_j}} & (i \neq j) \end{cases} \quad (1)$$

where  $i, j$  label scattering channels and  $\rho_i = 2p_{\text{cm},i}/E_{\text{cm}}$  is the phase space factor for channel  $i$ . The amplitudes show a cusp-like enhancement in  $\pi\eta \rightarrow \pi\eta$  near  $K\bar{K}$  threshold and a rapid turn on of amplitudes to  $K\bar{K}$ . This behaviour originates from an  $a_0(980)$ -like resonance which is strongly coupled to both  $\pi\eta$  and  $K\bar{K}$  – the first strongly-coupled meson-meson scattering system extracted in a lattice QCD calculation. The corresponding pole appears on a single unphysical Riemann sheet, unlike a canonical two-channel resonance where poles would be expected on two unphysical sheets, and this may be a sign that the state binds through the long-range interaction between a pair of mesons. Ref. [46] also presents results from including the  $\pi\eta'$  channel and considers  $D$ -wave scattering where a narrow tensor resonance is found.

Using a similar setup, in addition the HSC have recently determined the elastic  $\pi\pi$  S-wave  $I = 0$  scattering phase shift for the first time in a lattice QCD computation [47], work presented at this conference [20]. Two different light quark masses were used corresponding to  $m_\pi \approx 240$  MeV and 390 MeV. For the lighter mass the scattering amplitude has a pole on the unphysical Riemann sheet with a large imaginary part, corresponding to a broad resonance, in qualitative agreement with experiment. At the heavier mass a pole is found below threshold on the real axis of the physical sheet, corresponding to a bound state. Work is ongoing to extend this calculation into the coupled-channel region above  $K\bar{K}$  threshold where a  $f_0(980)$ -like resonance is expected, the final component of a study of the scalar meson nonet using lattice QCD.

<sup>3</sup>Note that  $\eta = 1$  would indicate no coupling between channels.

## 5 Heavy-light and charmonium-like resonances

Turning to channels relevant for heavy-light and quarkonium mesons, we begin with the charm-light ( $D$ ) and charm-strange ( $D_s$ ) sectors. The  $D_{s0}^*(2317)$  and  $D_{s1}(2460)$  present a long standing-puzzle: they were expected to be broad resonances, like the analogous  $D_0^*(2400)$  and  $D_1(2430)$  mesons, but were observed to be narrow states below the respective  $DK$  and  $D^*K$  thresholds [26]. Some early lattice calculations of elastic  $D^*\pi$  and  $D^*K$  scattering [48–50] were discussed elsewhere at this conference [51].

The HSC have recently investigated  $I = 1/2$  coupled-channel  $D\pi$ ,  $D\eta$ ,  $D_s\bar{K}$  scattering with light-quark masses corresponding to  $m_\pi \approx 390$  MeV on three lattice volumes [52]. Fig. 3 shows the  $S$ -wave scattering amplitudes constrained by 47 energy levels and Fig. 4 shows the locations of poles in the  $S$ -wave,  $P$ -wave and  $D$ -wave amplitudes. The broad feature in the  $D\pi \rightarrow D\pi$   $S$ -wave amplitudes is associated with a  $J^P = 0^+$  bound state very close to  $D\pi$  threshold. Although, by contrast, the associated experimental state,  $D_0^*(2400)$ , is a resonance, they are similar in that they influence a broad energy range and couple predominantly to  $D\pi$ . The pole position lies between what is observed experimentally for the  $D_{s0}^*(2317)$  and the  $D_0^*(2400)$ . In  $P$ -wave ( $J^P = 1^-$ ), a deeply bound state was found and can be compared to the experimentally observed narrow resonance,  $D^*(2007)$ . A narrow  $2^+$  resonance was found in  $D$ -wave. The  $I = 3/2$  elastic  $D\pi$  channel was also investigated and a weakly repulsive interaction found in  $S$ -wave.

Some preliminary results of the RQCD Collaboration's  $N_f = 2$  calculation of  $S$ -wave  $DK$  ( $J^P = 0^+$ ) and  $D^*K$  ( $1^+$ ) elastic scattering with light quarks corresponding to  $m_\pi = 150$  and 290 MeV were presented at this conference [53].

In the bottom sector, there have recently been lattice QCD investigations of near-threshold elastic  $B^{(*)}K$   $I = 0$  scattering with  $N_f = 2 + 1$  and  $m_\pi \approx 156$  MeV in a small volume – a bound state was found in both  $0^+$  and  $1^+$  [54]. In a study of  $I = 1$   $B_s\pi$ ,  $BK$  scattering, no sign was found of a  $X(5568)$  candidate [55]. These studies have been discussed elsewhere at this conference [51].

In the charmonium sector there have been a number of lattice QCD investigations [56–64]. However, the calculations are somewhat less advanced than in the other sectors and studies have generally been exploratory, inconclusive or have not determined the phenomena in detail or robustly, and I will not discuss these here. More robust and detailed computations are required – one challenge is the number of channels to which a resonance can potentially couple and all these channels need to be considered in the calculations.

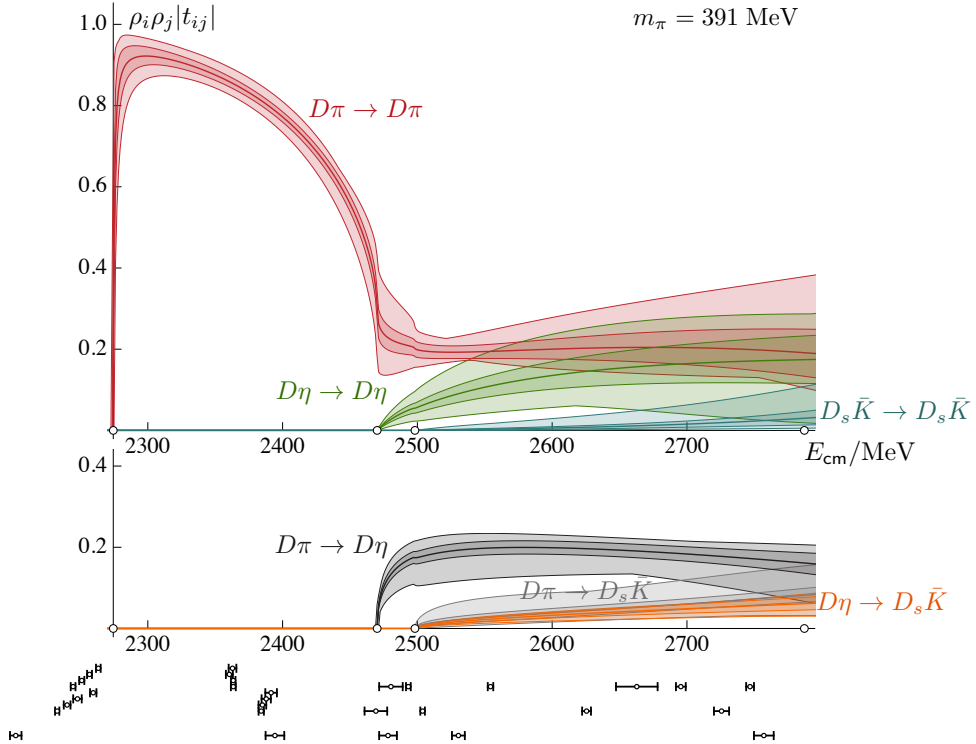


**Figure 3.** From Ref. [52]. The  $S$ -wave  $I = 1/2$   $D\pi$ ,  $D\eta$ ,  $D_s\bar{K}$  coupled-channel scattering amplitudes from a lattice calculation with  $m_\pi \approx 390$  MeV. Quantities proportional to the diagonal (off-diagonal) cross sections are plotted in the top (bottom) panel. Open circles on the horizontal axes indicate  $D\pi$ ,  $D\eta$ ,  $D_s\bar{K}$  and  $D^*\pi\pi$  thresholds. The black points below the plot show energy levels used to constrain the amplitudes.

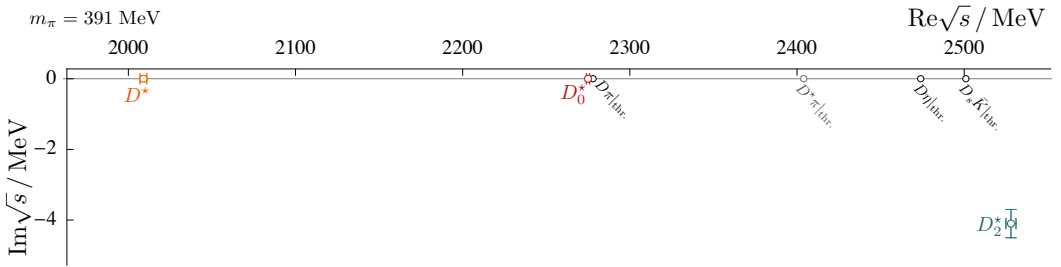


**Figure 4.** From Ref. [52]. Positions of poles in the complex energy plane,  $\sqrt{s} = E_{\text{cm}}$ , for  $S$ -wave ( $D_0^*$ ),  $P$ -wave ( $D^*$ ) and  $D$ -wave ( $D_2^*$ ) coupled-channel  $I = 1/2$   $D\pi$ ,  $D\eta$ ,  $D_s\bar{K}$  scattering. The black circles on the real axis indicate relevant thresholds.

## 6 Conclusions

I have presented some highlights of recent lattice QCD investigations of resonances and related scattering phenomena, an area which has seen significant advances in the last few years and where prospects for further progress are very good. Although many of the computations have used unphysically-heavy light quarks, corresponding to  $m_\pi$  larger than the physical value, and so cannot be compared quantitatively to experiment, studying how states evolve as  $m_\pi$  varies is a useful tool in discerning their nature. We have also seen the first calculation of a transition form factor involving a resonances, another handle which can be used to probe the structure of states.

As we go higher up in the spectrum and undertake calculations with  $m_\pi$  closer to the physical value, channels involving more than two hadrons will open up. Ongoing work on the formalism [65–70] for such situations has been discussed at this conference [71].

## Acknowledgements

I thank the organisers for the invitation to give a talk at this conference and my colleagues in the Hadron Spectrum Collaboration. I acknowledge support from the U.K. Science and Technology Facilities Council (STFC) [grant ST/L000385/1].

## References

- [1] M. Nielsen (2016), in these proceedings
- [2] S. Neubert (2016), in these proceedings
- [3] S. Durr et al., *Science* **322**, 1224 (2008), [0906.3599](#)
- [4] R. Dowdall, C. Davies, T. Hammant, R. Horgan, *Phys.Rev.* **D86**, 094510 (2012), [1207.5149](#)
- [5] C. Michael, *Nucl. Phys.* **B259**, 58 (1985)
- [6] M. Lüscher, U. Wolff, *Nucl. Phys.* **B339**, 222 (1990)
- [7] B. Blossier, M. Della Morte, G. von Hippel, T. Mendes, R. Sommer, *JHEP* **04**, 094 (2009), [0902.1265](#)
- [8] M. Lüscher, *Commun. Math. Phys.* **105**, 153 (1986)
- [9] M. Lüscher, *Nucl. Phys.* **B354**, 531 (1991)
- [10] M. Lüscher, *Nucl. Phys.* **B364**, 237 (1991)
- [11] K. Rummukainen, S.A. Gottlieb, *Nucl. Phys.* **B450**, 397 (1995), [hep-lat/9503028](#)
- [12] N.H. Christ, C. Kim, T. Yamazaki, *Phys.Rev.* **D72**, 114506 (2005), [hep-lat/0507009](#)
- [13] C. Kim, C. Sachrajda, S.R. Sharpe, *Nucl.Phys.* **B727**, 218 (2005), [hep-lat/0507006](#)
- [14] C. Liu, X. Feng, S. He, *Int. J. Mod. Phys.* **A21**, 847 (2006), [hep-lat/0508022](#)
- [15] Z. Fu, *Phys. Rev.* **D85**, 014506 (2012), [1110.0319](#)
- [16] L. Leskovec, S. Prelovsek, *Phys.Rev.* **D85**, 114507 (2012), [1202.2145](#)
- [17] M.T. Hansen, S.R. Sharpe, *Phys. Rev.* **D86**, 016007 (2012), [1204.0826](#)
- [18] R.A. Briceno, Z. Davoudi, *Phys. Rev.* **D88**, 094507 (2013), [1204.1110](#)
- [19] R.A. Briceno, *Phys. Rev.* **D89**, 074507 (2014), [1401.3312](#)
- [20] R. Briceño (2016), in these proceedings
- [21] S. Aoki et al. (CP-PACS), *Phys. Rev.* **D76**, 094506 (2007), [0708.3705](#)
- [22] X. Feng, K. Jansen, D.B. Renner, *Phys. Rev.* **D83**, 094505 (2011), [1011.5288](#)
- [23] C. Lang, D. Mohler, S. Prelovsek, M. Vidmar, *Phys.Rev.* **D84**, 054503 (2011), [1105.5636](#)
- [24] S. Aoki et al. (CS Collaboration), *Phys.Rev.* **D84**, 094505 (2011), [1106.5365](#)

- [25] C. Pelissier, A. Alexandru, Phys. Rev. **D87**, 014503 (2013), [1211.0092](#)
- [26] C. Patrignani et al. (Particle Data Group), Chin. Phys. **C40**, 100001 (2016)
- [27] D.J. Wilson, R.A. Briceno, J.J. Dudek, R.G. Edwards, C.E. Thomas, Phys. Rev. **D92**, 094502 (2015), [1507.02599](#)
- [28] J.J. Dudek, R.G. Edwards, M.J. Peardon, D.G. Richards, C.E. Thomas, Phys. Rev. **D82**, 034508 (2010), [1004.4930](#)
- [29] C.E. Thomas, R.G. Edwards, J.J. Dudek, Phys. Rev. **D85**, 014507 (2012), [1107.1930](#)
- [30] J.J. Dudek, R.G. Edwards, C.E. Thomas, Phys. Rev. **D86**, 034031 (2012), [1203.6041](#)
- [31] J.J. Dudek, R.G. Edwards, C.E. Thomas (Hadron Spectrum), Phys. Rev. **D87**, 034505 (2013), [Erratum: Phys. Rev. D90,no.9,099902(2014)], [1212.0830](#)
- [32] J. Bulava, B. Fahy, B. Hörz, K.J. Juge, C. Morningstar, C.H. Wong, Nucl. Phys. **B910**, 842 (2016), [1604.05593](#)
- [33] G.S. Bali, S. Collins, A. Cox, G. Donald, M. Göckeler, C.B. Lang, A. Schäfer (RQCD), Phys. Rev. **D93**, 054509 (2016), [1512.08678](#)
- [34] D. Guo, A. Alexandru, R. Molina, M. Döring, Phys. Rev. **D94**, 034501 (2016), [1605.03993](#)
- [35] B. Hu, R. Molina, M. Döring, A. Alexandru, Phys. Rev. Lett. **117**, 122001 (2016), [1605.04823](#)
- [36] R. Molina, D. Guo, B. Hu, A. Alexandru, M. Doring (2016), [1611.04536](#)
- [37] A. Agadjanov, V. Bernard, U.G. Meißner, A. Rusetsky, Nucl. Phys. **B886**, 1199 (2014), [1405.3476](#)
- [38] R.A. Briceño, M.T. Hansen, A. Walker-Loud, Phys. Rev. **D91**, 034501 (2015), [1406.5965](#)
- [39] R.A. Briceño, M.T. Hansen, Phys. Rev. **D92**, 074509 (2015), [1502.04314](#)
- [40] L. Lellouch, M. Luscher, Commun. Math. Phys. **219**, 31 (2001), [hep-lat/0003023](#)
- [41] R.A. Briceno, J.J. Dudek, R.G. Edwards, C.J. Shultz, C.E. Thomas, D.J. Wilson, Phys. Rev. Lett. **115**, 242001 (2015), [1507.06622](#)
- [42] R.A. Briceño, J.J. Dudek, R.G. Edwards, C.J. Shultz, C.E. Thomas, D.J. Wilson, Phys. Rev. **D93**, 114508 (2016), [1604.03530](#)
- [43] J.J. Dudek, R.G. Edwards, C.E. Thomas, D.J. Wilson (Hadron Spectrum), Phys. Rev. Lett. **113**, 182001 (2014), [1406.4158](#)
- [44] D.J. Wilson, J.J. Dudek, R.G. Edwards, C.E. Thomas, Phys. Rev. **D91**, 054008 (2015), [1411.2004](#)
- [45] J. Nebreda, J.R. Pelaez, Phys. Rev. **D81**, 054035 (2010), [1001.5237](#)
- [46] J.J. Dudek, R.G. Edwards, D.J. Wilson (Hadron Spectrum), Phys. Rev. **D93**, 094506 (2016), [1602.05122](#)
- [47] R.A. Briceno, J.J. Dudek, R.G. Edwards, D.J. Wilson (2016), [1607.05900](#)
- [48] D. Mohler, S. Prelovsek, R.M. Woloshyn, Phys. Rev. **D87**, 034501 (2013), [1208.4059](#)
- [49] D. Mohler, C.B. Lang, L. Leskovec, S. Prelovsek, R.M. Woloshyn, Phys. Rev. Lett. **111**, 222001 (2013), [1308.3175](#)
- [50] C.B. Lang, L. Leskovec, D. Mohler, S. Prelovsek, R.M. Woloshyn, Phys. Rev. **D90**, 034510 (2014), [1403.8103](#)
- [51] D. Mohler (2016), in these proceedings
- [52] G. Moir, M. Peardon, S.M. Ryan, C.E. Thomas, D.J. Wilson, JHEP **10**, 011 (2016), [1607.07093](#)
- [53] G. Bali (2016), in these proceedings
- [54] C.B. Lang, D. Mohler, S. Prelovsek, R.M. Woloshyn, Phys. Lett. **B750**, 17 (2015), [1501.01646](#)
- [55] C.B. Lang, D. Mohler, S. Prelovsek, Phys. Rev. **D94**, 074509 (2016), [1607.03185](#)
- [56] S. Ozaki, S. Sasaki, Phys. Rev. **D87**, 014506 (2013), [1211.5512](#)

- [57] S. Prelovsek, L. Leskovec, Phys. Rev. Lett. **111**, 192001 (2013), [1307.5172](#)
- [58] S. Prelovsek, L. Leskovec, Phys. Lett. **B727**, 172 (2013), [1308.2097](#)
- [59] S. Prelovsek, C.B. Lang, L. Leskovec, D. Mohler, Phys. Rev. **D91**, 014504 (2015), [1405.7623](#)
- [60] Y. Chen et al., Phys. Rev. **D89**, 094506 (2014), [1403.1318](#)
- [61] M. Padmanath, C.B. Lang, S. Prelovsek, Phys. Rev. **D92**, 034501 (2015), [1503.03257](#)
- [62] C.B. Lang, L. Leskovec, D. Mohler, S. Prelovsek, JHEP **09**, 089 (2015), [1503.05363](#)
- [63] Y. Chen et al. (CLQCD), Phys. Rev. **D92**, 054507 (2015), [1503.02371](#)
- [64] T. Chen et al. (CLQCD), Phys. Rev. **D93**, 114501 (2016), [1602.00200](#)
- [65] S.R. Beane, W. Detmold, M.J. Savage, Phys. Rev. **D76**, 074507 (2007), [0707.1670](#)
- [66] K. Polejaeva, A. Rusetsky, Eur. Phys. J. **A48**, 67 (2012), [1203.1241](#)
- [67] R.A. Briceno, Z. Davoudi, Phys. Rev. **D87**, 094507 (2013), [1212.3398](#)
- [68] M.T. Hansen, S.R. Sharpe, Phys. Rev. **D90**, 116003 (2014), [1408.5933](#)
- [69] M.T. Hansen, S.R. Sharpe, Phys. Rev. **D92**, 114509 (2015), [1504.04248](#)
- [70] M.T. Hansen, S.R. Sharpe, Phys. Rev. **D93**, 014506 (2016), [1509.07929](#)
- [71] M. Hansen (2016), in these proceedings